

# SHAPED NONIMAGING FRESNEL LENSES

Ralf Leutz<sup>\*†</sup>, Akio Suzuki<sup>\*\*</sup>, Atsushi Akisawa<sup>\*</sup> and Takao Kashiwagi<sup>\*</sup>

<sup>\*</sup>Tokyo University of Agriculture and Technology,  
Department of Mechanical Systems Engineering  
2-24-16 Naka-cho, Koganei-shi, Tokyo 184-8588, Japan  
<sup>†</sup> email ralf@star.cad.mech.tuat.ac.jp, phone/fax +81-42-388-7076

<sup>\*\*</sup>UNESCO,  
SC/EST, 1, rue Miollis, 75732 Paris Cedex 15, France

**Abstract** – Shaped nonimaging Fresnel lenses have been designed according to the edge ray principle, incorporating any combination of two acceptance half angle pairs. A numerical solution yields nonimaging lenses consisting of minimum deviation prisms. If the outer surface of the lens must be smooth, the lens shape will be convex. A linear lens prototype intended as concentrator for the collection of solar energy has been designed, manufactured and tested. Results in terms of flux distribution and optical concentration ratio are presented. Shaped nonimaging Fresnel lenses are suited for application as solar concentrators, or as collimators, or in lighting applications, where they can fulfil technological requirements as well as being adaptable to the necessities of fashionable design.

## Nonimaging Fresnel Lenses

Nonimaging optics have become an integral part of optical technologies. Various nonimaging solutions in diverse fields such as optical transmission of communication, pumping of lasers, or the collection of solar energy are widely employed. Virtually all present nonimaging concentrators work on the principle of reflection, i.e. they involve mirrors to concentrate or guide radiation.

This paper presents shaped nonimaging lenses, i.e. refractive devices following a given form. Refraction, or the use of lenses does suit itself for the use of nonimaging design principles. In particular, an optimum nonimaging lens with smooth outer surface has been created, and was manufactured and tested as solar concentrator of medium concentration ratio.

Nonimaging design depends primarily on the edge ray principle (Welford and Winston, 1989), which describes an optical system by means of rays entering its first (entry) aperture. Should the nonimaging system be ideal, the extreme rays of the entry aperture are passing the optical system's second (exit) aperture likewise as extreme rays. Ideal means that all radiation entering the system at angles smaller than those of the edge rays, will exit the system within the boundaries of the exiting edge rays.

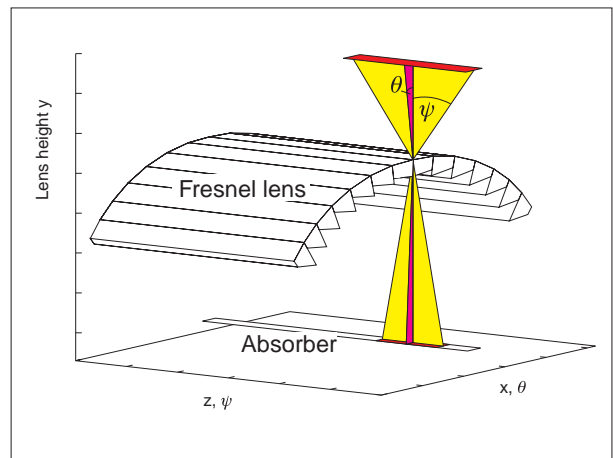


Figure 1: Nonimaging linear Fresnel lens solar concentrator. Schematic of acceptance half angles: cross-sectional  $\theta$  and perpendicular  $\psi$ .

Of great practical importance is the design of nonimaging concentrator systems, where the exit aperture is smaller than the entry aperture by a concentration factor  $1/C$ . It has been shown that a linear Compound Parabolic Concentrator (CPC) can achieve ideal concentration at  $C = 1/\sin \theta$ , where  $\theta$  is the cross-sectional acceptance half angle, or the angle between the first edge ray and the collector's optical axis. Welford and Winston (1989) also prove that the CPC of rotational symmetry ( $C = 1/\sin^2 \theta$ ) is not

ideal, on account of some skew rays being reflected back through the entry aperture. If the first aperture of the ideal concentrator is completely filled out by uniform light (a Lambertian source), the second aperture will receive uniform flux.

Nonimaging systems do not create an image and do not have a focus. Optical aberrations are similar, but not equal to those observed in imaging systems. Nonimaging optics are treated like geometrical optics, and ray tracing is the tool for their evaluation.

Refraction, or the design of lenses may take advantage of nonimaging principles. Lenses are superior to mirrors in respect of the prisms' partial self correction of slope errors, the refracted ray is affected little, while the reflected ray's direction angle is changed by double the slope misorientation. New plastic materials for lenses offer high transmittance and durability for common wavelengths, while keeping the system inexpensive and lightweight.

Nonimaging lenses have rarely been designed — to our knowledge, only three times in the past: by Collares-Pereira (1979), at the same time by Kritchman *et al.* (1979), and slightly later by Lorenzo and Luque (1981). (Most probably, the late W. T. Welford deserves the honour to be credited with the initial idea for the design of curved nonimaging lenses.) All these lenses were intended for the collection of solar energy, where photographic accuracy is of no importance, as long as radiation can be captured. None of the lenses had actually been built, and their design lacks two characteristics, namely a secondary acceptance half angle  $\psi$  perpendicular to  $\theta$  (although the lenses were propositioned as linear concentrators); and the use of minimum deviation prisms. The former is necessary to account for refraction in the perpendicular plane, the latter minimizes optical losses, in particular the chances for total internal reflection.

O'Neill (1978) designed an imaging lens, but realized that his lens could compensate for tracking errors and errors due to the size of the solar disk within narrow limits. In contrast to nonimaging designs, this lens is characterized by a deliberately 'sloppy' approach. O'Neill's lens is the only Fresnel lens for solar energy applications that, first, had been designed solely for this purpose, and second, has been commercially somewhat successful.

The nonimaging Fresnel lenses presented in the present paper are designed (Leutz *et al.* (1999a)) as optimum lenses for linear concentration of solar energy, and for any systems where the lens should roughly equal a collimator, such as lighting applications. The design incorporates any acceptance half angles  $\theta$  and  $\psi$ , depending on what concentration ra-

tio is to be achieved, accounting for tracking requirements, and errors due to the size of the solar disc. Minimum deviation prisms of finite size constitute for the Fresnel lens. The absorber has a finite size; two solid angles of light are translated into each other, a fraction of the sky 'seen' by the lens is refracted onto the solar receiver, or the size of the light source is refracted into an area to be lit. The lens can be used in a reversible way.

## Nonimaging Lens Design

A schematic of the working principle of the nonimaging linear Fresnel lens depicting the cross-sectional acceptance half angle  $\theta$ , and its perpendicular counterpart  $\psi$  is shown in Fig.1. The edge rays in the entry aperture (rays entering the lens surface at maximum combinations of the design angles), are refracted by each prism so that they exit the second aperture at the corners of the illuminated field on the absorber. Graphically, an upside-down pyramid of light enters the lens, and is refracted towards the absorber. The lens can be designed as being of rotational symmetry, the perpendicular design angle  $\psi$  then is set to zero.

The design process determining the prism inclination  $\alpha$ , the prism angle  $\beta$ , and the prism's location relative to the absorber has been described in detail in Leutz *et al.* (1999a). The main design steps are as follows, referring to Fig.2.

As opposed to imaging Fresnel lenses where the distance between lens and focused image is determined by  $f/number$  and the lensmaker's formula, absorber half width  $d$  and height of the nonimaging lens above the absorber are related by  $y_0 = d/\tan\theta$ . This assumes the prism on the optical axis to be thin. In practice the innermost prisms are approximately flat plates.

From this point, a prism is determined with the help of the acceptance half angle pair  $\pm\theta$  describing (asymmetrical) incidence from the left and the right on the prism and the symmetrical acceptance half angle  $\psi$ . Only the right side of the lens is determined, the left side is later constructed as mirrored version. A set of vectors representing the incidence from left and right on their paths of double refraction through the prism  $\vec{q}^{+\theta\psi}$  and  $\vec{q}^{-\theta\psi}$  is derived. These vectors represent the extreme rays of the edge ray principle.

The two edge ray vectors depend on the prism inclination  $\alpha$ , and the prism angle  $\beta$ . Two conditions are to be fulfilled: the outer surface of the lens should be smooth (or the lens shape must follow an otherwise clearly defined function); and the prisms designed

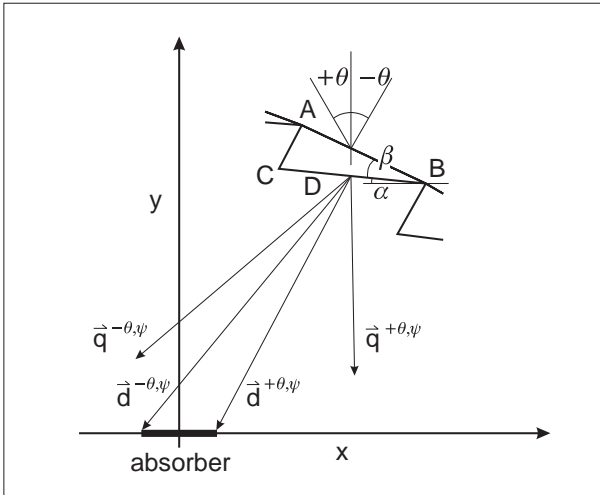


Figure 2: Evaluating the prism position relative to the absorber. Refracted edge rays for incidence from both sides, and depending on  $\psi$  (vectors  $\vec{q}^{+\theta\psi}$  and  $\vec{q}^{-\theta\psi}$ ) are compared with the prism position vectors relative to either end of the absorber  $\vec{d}^{+\theta\psi}$  and  $\vec{d}^{-\theta\psi}$ . The vectors  $\vec{q}$  are plotted to scale, the vectors  $\vec{d}$  are not. Projection into cross-sectional plane.

should be minimum deviation prisms for minimized optical losses, and minimum dispersion. The maximum height  $y_0$  of the lens over the absorber is found for the point of intersection of lens and optical axis of the system:  $y_0 = 1/\tan\theta$ .

No analytical solution can be found for prism angle and prism inclination, should the two conditions of defined surface and minimum deviation be fulfilled, and no further assumptions be made. In the numerical solution, two nested infinity loops are programmed, and solved with the help of Newton's Method. In the inner loop, the prism angle  $\beta$  is decided upon once both directions of design incidence ( $+\theta, \psi$  and  $-\theta, \psi$ ; the edge rays) yield prism angles identical within an error margin.

The outer loop compares the two vectors  $\vec{q}^{+\theta\psi}$  and  $\vec{q}^{-\theta\psi}$  pictured in Fig.2 with the location of the prism stated by the vectors  $\vec{d}^{+\theta\psi}$  and  $\vec{d}^{-\theta\psi}$ . Once the vectors  $\vec{d}$  and  $\vec{q}$  are found to be parallel within a confidence interval, the prism inclination  $\alpha$  is fixed.

It should be noted that Fig.2 is a two-dimensional, cross-sectional projection of the procedure outlined. The influence of the perpendicular angle  $\psi$  is incorporated in the design, but can hardly be traced in said figure.

Subsequently, the next prism is found feeding its numerical optimization procedure with the values of the previous prism. Once the next prism would reach

the level of the absorber, or any other break criterion, the simulation is stopped. In order to achieve finite thickness of the lens, prisms are designed partly overlapping previous ones.

The symmetry in the incidence angles  $\pm\theta$  and  $\psi$  determining the vectors  $\vec{d}^{\pm\theta\psi}$  reaching the edges of the symmetrical absorber, as well as the quasi-symmetry in splitting the design of the prism into the calculation of two dependent angles  $\alpha$  and  $\beta$  results in the creation of prisms that are close to minimum deviation prisms.

Of course, one prism can have only one angle of minimum deviation, but the design described here yields paths for both edge rays that are reversible. The edge rays enter the prism at an angle  $\phi$ , with its cross-sectional component dictated by the design half angles  $\pm\theta$ , and the perpendicular component set by the secondary acceptance half angle  $\psi$ .

For the maximum angle of incidence on the first surface from the left side  $\phi_1^{+\theta\psi}$ , an angle of refraction on the second surface  $\phi_2^{+\theta\psi}$  is recorded, where the latter approximately coincides with the angle of maximum incidence from the right side  $\phi_1^{-\theta\psi}$ , and the former roughly equals the angle of refraction for incidence from the right side on the second surface  $\phi_2^{-\theta\psi}$ .

Although minimum deviation happens only for one angle of incidence on each prism, symmetrical paths and the principle of the reversibility of light are the basic concepts of minimum deviation, the 'reversible' prisms described here are to be called minimum deviation prisms.

## Lens Shapes

The starting point  $A$  for each subsequent prism can be chosen so that the prisms follow a predefined lens shape. Point  $A$  may be found as  $y = f(x)$ , where the mathematical function must fulfil two conditions. First, the slope of the function must allow the refracted light to reach the absorber, thus the tangents at any point must be smaller than one, with the absorber assumed to be small. The outermost prisms following function  $c$  in Fig.3, and in lens  $c$  in Fig.4 are problematic in this respect. Second, the function must pass through the previously found  $y_0$ , according to the edge ray principle.

Though not impossible, three-dimensional functions are to be avoided for practical reasons. Prisms would change their shape according to  $y = f(x, z)$ , and manufacturing would be a difficult task. One may understand the linear lenses in Fig.4 as representing various cross-sections at different depths  $z$  of

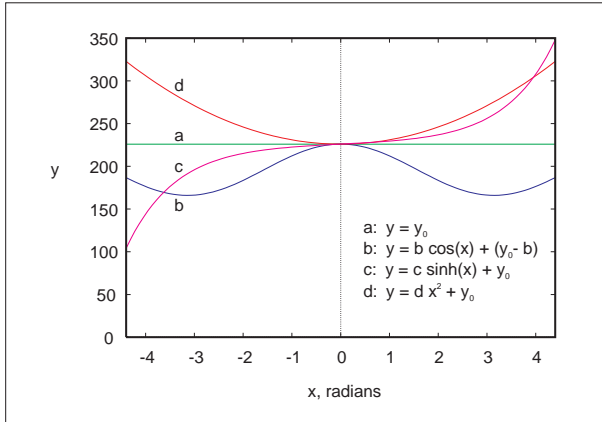


Figure 3: Functions used to design shaped nonimaging Fresnel lenses.

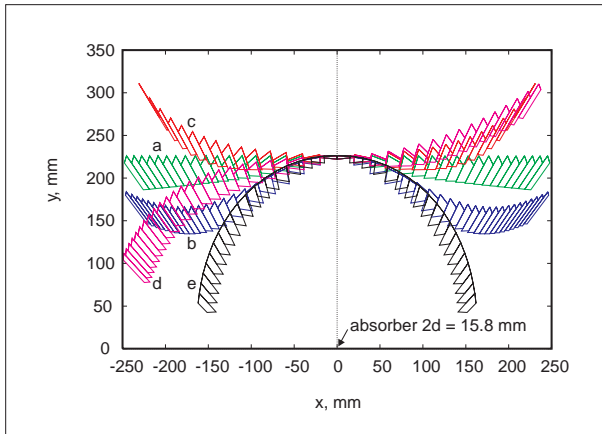


Figure 4: Shaped nonimaging Fresnel lenses following functions. Acceptance half angle pairs  $\pm\theta = 2^\circ$  in the cross-sectional plane (the plane of the paper), and  $\pm\psi = 12^\circ$  in the plane perpendicular to it. Oversized prisms. Lens  $e$  is the optimum lens shape, where a smooth outer surface was required. The previously manufactured prototype of  $e$  is truncated at  $y = 1/2y_0$ .

one lens wavering over a flat absorber like a blanket in the wind. Three-dimensional lenses of rotational symmetry can easily be obtained by setting the perpendicular acceptance half angle  $\psi = 0$ .

The lenses in Fig.4 are all designed taking into account the same acceptance half angle pairs  $\pm\theta = 2^\circ$  in the cross-sectional plane (the plane of the paper), and  $\pm\psi = 12^\circ$  in the plane perpendicular to it. The design of each prism follows the edge ray principle represented by the vectors  $\vec{q}^{+\theta\psi}$  and  $\vec{q}^{-\theta\psi}$ . Acceptance half angles and absorber size have been chosen to equal those of a prototype previously manufactured. This

prototype has been plotted as lens  $e$  in Fig.4, with the difference that the prototype is truncated at  $y = 1/2y_0$ .

For greater acceptance half-angles the lens moves closer to the absorber: i.e. if the distance between the center of the lens and the absorber is to be kept constant, the absorber width will increase. Likewise, the curvature of an optimum lens with greater acceptance half angles will become softer.

Shapes other than that of the optimum lens curved over the absorber, like flat, or concave forms are sub-optimal in concentrating white light incident from both the left and right. The shape of a lens may be desirable for on account of its smooth integration into existing shapes. Solar collectors may fit architectural designs, such as daylighting, or lenses for lamps should suit lighting designs, for example. Erismann (1997) designed a Fresnel lens, which is inherently aspherical, following a spherical shape for a infrared sensor, for reasons of fashion.

### Performance of Shaped Lenses

The optical performances of the nonimaging Fresnel lenses are evaluated by ray tracing. Geometrical losses at the lens are described in detail in Leutz *et al.* (1999a). Losses due to the refractive influence of the perpendicular acceptance half angle  $\psi$  are shown in Fig.5. Some rays incident at combinations of  $\theta_{in}$  and  $\psi_{in} < \psi$  are missing the absorber, due to the refractive influence of the perpendicular incidence. In order to minimize absorber misses, it is essential to keep the relation between the design angles  $\theta$  and  $\psi$  reasonable, well within one order of magnitude.

Incident light may be covering a range of wavelengths, e.g. in the case of sunlight. Nonimaging Fresnel lenses are partially mixing the dispersed refracted rays on the absorber plane, due to incidence from both sides of the lens. This leads to a relatively homogeneous color distribution (Leutz *et al.*, 1999b).

For a single combination of incidence within the acceptance half angles ( $\theta_{in} < \theta$ ,  $\psi_{in} < \psi$ ), there exists nonhomogeneous illumination on the absorber, i.e. a 'hot spot' is formed. This is expected as long as the entry aperture is not filled out completely with homogeneous radiation. A typical distribution of flux on the absorber at a prototype lens of  $\pm\theta = 2^\circ$  and  $\pm\psi = 12^\circ$  has recently been measured and simulated. The prototype follows the discription of lens  $e$  above, including truncation. The experimental setup including the lens and a device to measure radiation flux is shown in Fig.6.

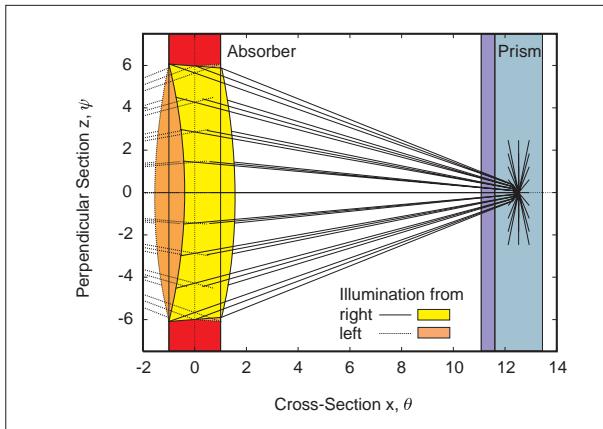


Figure 5: Top view of exemplary prism and absorber of the nonimaging Fresnel lens with acceptance half angle pairs  $\pm\theta = 2^\circ$  and  $\pm\psi = 12^\circ$ . Incident light at  $\theta_{in}$ ,  $\psi_{in}$  fills out an upside-down pyramid on any point of the lens, is refracted twice at the prism's faces, and shown intersecting the absorber level, where rays form a curved band of light due to perpendicular refraction. Oversized prism, for yellow light, refractive index  $n = 1.49$  (Polymethylmethacrylate, PMMA).

The experiment is rather crude, the main problems being the exact orientation in relation to the apparently moving sun, and the relatively large size of the flux meter's window. In spite of that, a good agreement of simulated and measured flux on the absorber of the prototype lens for normal incidence  $\theta_{in} = \psi_{in} = 0^\circ$  can be observed in Fig.7. The measured curve appears shifted for reasons of misorientation. The 'hot spot' of the simulated flux distribution cannot be followed by the flux meter due to its window size.

Direct solar radiation during the flux experiment was approximately  $750 \text{ W/m}^2$ , while total radiation did not exceed  $915 \text{ W/m}^2$ . Distortions due to diffuse radiation (which is not considered in the model) are negligible.

Interestingly, the lenses  $a - d$  are characterized by a slightly more narrow 'hot spot' than the optimum shaped lens  $e$ , due to the latter's design inherent non-ideal behaviour of the outermost prisms, which in the extreme case may be shaded for part of the incidence. The closer definition of the focal area observed with the lenses  $a - d$  is true only for monochromatic light. If dispersion occurs, the performance increasingly suffers for prisms that are relatively distant to the absorber.

Nonimaging Fresnel lenses can be built as 'fast' lenses, i.e. their  $f/\text{number} < 1.0$ . Where the condi-



Figure 6: Experimental setup to measure the radiation flux distribution of a linear nonimaging Fresnel lens with acceptance half angle pairs of  $\pm\theta = 2^\circ$ , and  $\pm\psi = 12^\circ$ . The lens is intended as solar concentrator for photovoltaic applications. Lens length is 400 mm. 30 July 1999, Tokyo, Japan.

tion of a smooth outer surface does not restrict this parameter, dispersion will act as a limit.

The performance of any collector system incorporating a concentrator may be described in terms of radiation reaching the absorber. In contrast to the flux density which describes intensity and distribution of the radiation on the absorber, the optical performance of the lens itself may be described by the optical concentration ratio. The optical concentration ratio is understood as the ratio of angular radiation intensity after having passed the lens, and thereafter passing through the second aperture, to the radiation intensity of identical radiation that has not been interfered with. The optical concentration ratio is calculated as product of geometrical concentration ratio and optical efficiency, incorporating geometrical losses, absorber misses, and optical losses (first order reflection).

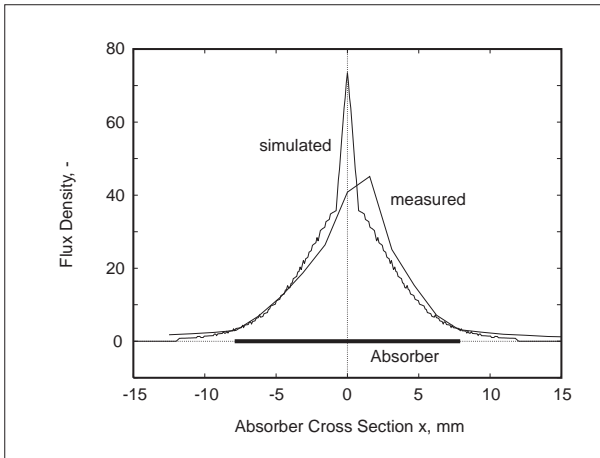


Figure 7: Simulated and measured relative radiation flux on the absorber of a linear nonimaging Fresnel lens with acceptance half angle pairs of  $\pm\theta = 2^\circ$ , and  $\pm\psi = 12^\circ$  for normal incidence  $\theta_{in} = \psi_{in} = 0^\circ$ . 30 July 1999, Tokyo, Japan.

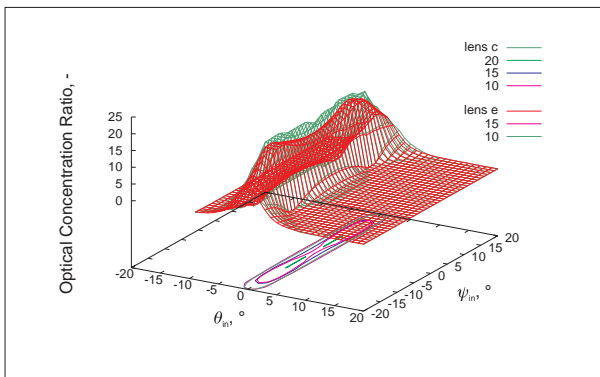


Figure 8: Optical concentration ratios of nonimaging Fresnel lenses  $c$  and  $e$  with acceptance half angle pairs of  $\pm\theta = 2^\circ$ , and  $\pm\psi = 12^\circ$ .

The optical concentration ratio of nonimaging devices is characterized by a sharp drop once the incidence angles exceed the design acceptance half angles, and the refracted rays miss the absorber, as shown in Fig. 8. In this figure the optical concentration ratios of the lenses  $c$  and  $e$  are compared. Lens  $c$  extends further, and intercepts more radiation incident at design angles. Both lenses require approximately the same amount of material when produced as flat sheet lenses. Note that the size of practically used prisms is reduced to less than 1.0 mm, as opposed to Fig. 4.

The advantage of the optimum shaped lens  $e$  is its smooth outer surface facilitating manufacturing, and the use of the lens without cover, as cleaning is possible.

## Conclusions

The principles of nonimaging optics have been successfully applied to the design of a novel class of nonimaging Fresnel lenses. The edge ray principle allows for the creation of nonimaging lenses with any combination of acceptance half angles  $\theta$  in the cross-sectional plane, and  $\psi$  in the plane perpendicular to it. Minimum deviation prisms constitute for the lens, solutions are found in a numerical simulation. The concentrator lens is nonideal for any design angle  $\psi > 0$ .

Optimum nonimaging Fresnel lenses may have any shape. If the lens should have a smooth outer surface, its shape is convex. The realization of lenses without one smooth side is likely to be restricted by present manufacturing technologies.

A prototype linear concentrator intended for the collection of solar energy has been manufactured. Test results, and simulated performance show good agreement. The ‘hot spot’ is of modest nature, and depends strongly on the wavelength components of the incident radiation. If white light (e.g. sunlight) is available, dispersed colors are mixed on the absorber, and flux distribution is more homogeneous. Some rays, however, will miss the absorber; due to dispersion and due to the influence of the design angle  $\psi$ .

Nonimaging Fresnel lenses can be designed as ‘fast’ lenses. Besides the initial success of their use in solar energy applications as collector of medium concentration for photovoltaics, lenses of various shapes can be integrated with architectural and technological requirements. A large field of anticipated applications is the use of the novel nonimaging lens as collimator, or reversed concentrator for lighting.

## Acknowledgement

The financial support of the Solar Fresnel Lens Project by the Japanese Science and Technology Corporation is gratefully acknowledged.

## References

- M. Collares-Pereira (1979) High Temperature Solar Collector with Optimal Concentration: Non-Focusing Fresnel Lens with Secondary Concentrator; *Solar Energy* **23**, 409-420
- F. Erisman (1997) Design of plastic aspheric Fresnel lens with a spherical shape *Opt. Eng.* **36**, 4, 988-991; also available from <http://www.wavelengthoptics.com/techpap1.htm>

- E. M. Kritchman, A. A. Friesem, G. Yekutieli (1979) Efficient Fresnel Lens for Solar Concentration; *Solar Energy* **22**, 119-123
- R. Leutz, A. Suzuki, A. Akisawa, T. Kashiwagi (1999a) Design of a Nonimaging Fresnel Lens for Solar Concentrators; *Solar Energy*, **65**, 6, 379-388
- R. Leutz, A. Suzuki, A. Akisawa, T. Kashiwagi (1999b) Nonimaging Fresnel Lens Concentrators for Photovoltaic Applications; *Proceedings of the ISES Solar World Congress*, 4-9 July, Jerusalem, Israel
- E. Lorenzo, A. Luque (1981) Fresnel Lens Analysis for Solar Energy Applications; *Applied Optics* **20**, 17, 2941-2945
- M. J. O'Neill (1978) Solar Concentrator and Energy Collection System; United States Patent 4069812
- W. T. Welford, R. Winston (1989) High Collection Nonimaging Optics, San Diego